LIGHTCURVE ANALYSIS FOR EIGHT NEAR-EARTH ASTEROIDS

Peter Birtwhistle
Great Shefford Observatory
Phlox Cottage, Wantage Road
Great Shefford, Berkshire, RG17 7DA
United Kingdom
peter@birtwhistle.org.uk

(Received: 2022 October 12)

Lightcurves and amplitudes for eight near-Earth asteroids observed from Great Shefford Observatory during close approaches between 2022 July and September are reported. All are superfast rotators, with periods < 12 minutes and three are identified as tumblers, i.e., showing non-principal axis rotation.

Photometric observations of near-Earth asteroids during close approaches to Earth between 2022 July and September were made at Great Shefford Observatory using a 0.40-m Schmidt-Cassegrain and Apogee Alta U47+ CCD camera. All observations were made unfiltered and with the telescope operating with a focal reducer at *f*/6. The 1K×1K, 13-micron CCD was binned 2×2, resulting in an image scale of 2.16 arc seconds/pixel. All the images were calibrated with dark and flat frames and *Astrometrica* (Raab, 2018) was used to measure photometry using APASS Johnson V band data from the UCAC4 catalogue (Zacharias et al., 2013). *MPO Canopus* (Warner, 2022), incorporating the Fourier algorithm developed by Harris (Harris et al., 1989), was used for lightcurve analysis.

No previously reported results for any of the objects reported here have been found in the Asteroid Lightcurve Database (LCDB) (Warner et al., 2009), from searches via the Astrophysics Data System (ADS, 2022), or from wider searches unless otherwise noted. All size estimates are calculated using *H* values from the Small-Body Database Lookup (JPL 2022), using an assumed albedo for NEAs of 0.2 (LCDB readme.pdf file) and are therefore uncertain and offered for relative comparison only.

2022 NE. This small Apollo, with $H = 28.7$ implying a diameter of ~ 6 m was discovered by the Pan-STARRS2 team on 2022 July 4 at 20th mag, 51 hours before passing Earth at 0.4 Lunar Distances (LD) (Evans et al., 2022). It was observed for 45 minutes starting at 2022 July 5.98 UTC when it was at magnitude 17 and at a range of 1.1 LD. With an apparent speed of 80 - 90 arcsec/min. exposures were limited to 4.5 - 5 sec to keep trailing of the target within the measurement annulus used in *Astrometrica*. An initial analysis in *MPO Canopus* indicated a fast rotation period of 55.8 sec, but with a larger than expected scatter in the lightcurve, with the RMS being 0.31 mags. The lightcurve is given here labelled PAR, i.e., Principal Axis Rotation assumed. However, multiple potential solutions are apparent in the period spectrum, which is plotted on a linear scale for periods between 18 - 155 s. It is noted there are three apparent sets of four equally spaced minima, the strongest signal from multiples of 27.9 s, the next strongest from multiples of 36.1 s and the weakest from multiples of 21.9 s.

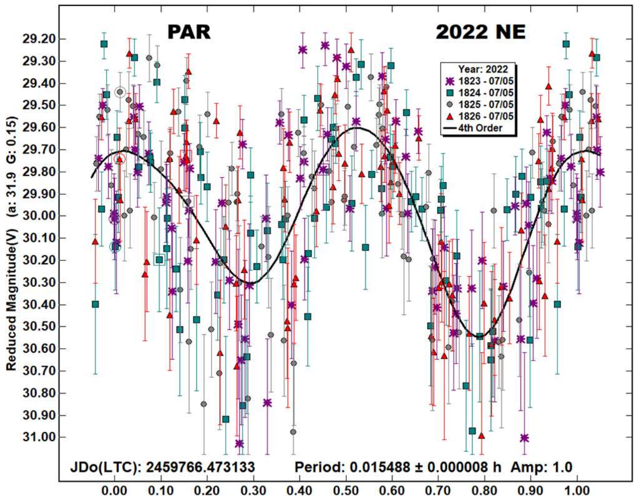

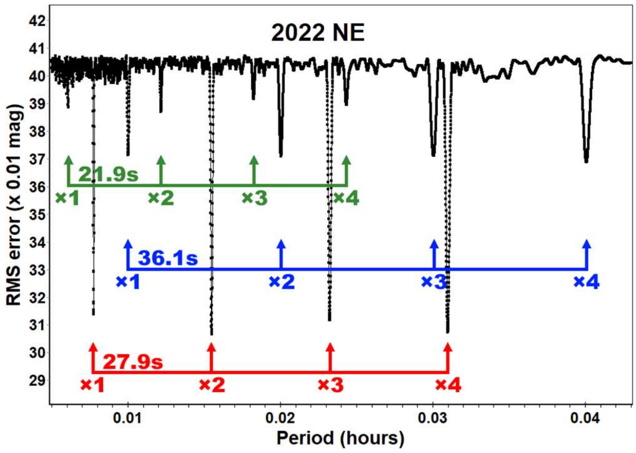

It was suspected that non-principal axis (NPA) rotation, or tumbling may be present and so the Dual-Period search function in *MPO Canopus* was used to try and identify the possible values for rotation and precession. This resolved two periods, $P_1 = 0.015488 \pm 0.000004$ h and $P_2 = 0.02005 \pm 0.00001$ h as providing the best fit to the observations, reducing the overall RMS to 0.25 mag. However, solutions were also possible using either the P_1 or P_2 value as a starting point in the dual period search, both searches isolating a period $P_3 \sim 0.01217$ h, with slightly poorer RMS values, the three pairs of solutions summarised here:

$P_1 = 0.015488 \pm 0.000004$ h and $P_2 = 0.02005 \pm 0.00001$ h, RMS = 0.25
$P_1 = 0.015487 \pm 0.000005$ h and $P_3 = 0.01217 \pm 0.00001$ h, RMS = 0.28
$P_2 = 0.02004 \pm 0.00002$ h and $P_3 = 0.01216 \pm 0.00001$ h, RMS = 0.35

Periods P_1, P_2 and P_3 match minima in the period spectrum marked as ×2 multiples, i.e., 55.8, 72.2 and 43.8 s respectively and all produce bimodal lightcurves. It is noted that the frequencies are related to each other, where $1/P_1 \approx 2/P_3 - 2/P_2$. The real periods of rotation and precession cannot be resolved from this analysis; one of the three periods will be an alias but it is not clear which one. It is expected that 2022 NE may be rated with a PAR code of -3 on the scale of Pravec et al. (2005), i.e., *NPA rotation reliably detected with the two periods resolved. An ambiguity of the periods solution may be tolerated provided the resulting spectrum of frequencies with significant signal is the same for the different solutions.* Lightcurves from the best fit solution for periods P_1 and P_2 are given and a lightcurve for period P_3 from the P_1 and P_3 solution is also given.

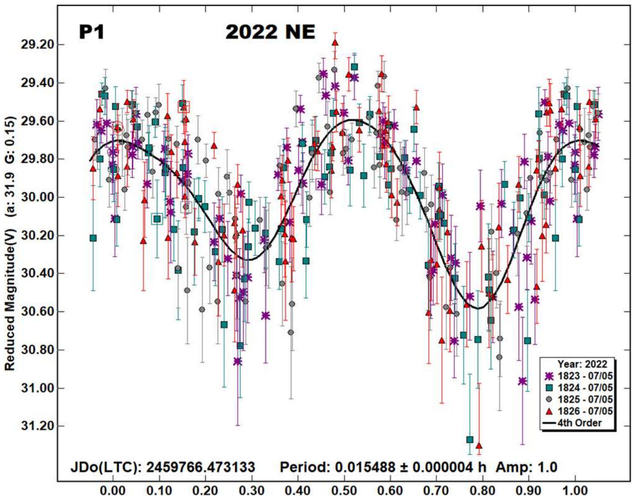

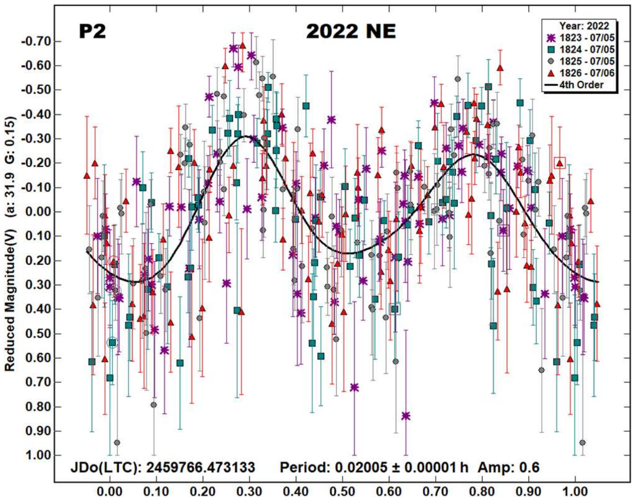

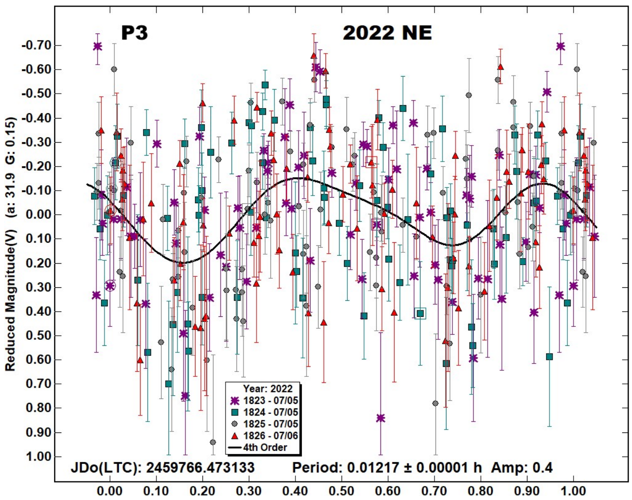

2022 NR. The Catalina Sky Survey's 0.68-m Schmidt picked this Apollo up at 18th mag on 2022 July 6.3 UTC, some four days before it passed Earth at 1 LD (Fazekas et al., 2022). With H = 25.8, its size is estimated at ~20 m. It was observed on 2022 July 7.9 UTC for 15 minutes to measure astrometry when it was still mag +18 and then for 2.5 h the next night when it had brightened to mag +17. By then its apparent speed was 40 arcsec/min and exposures were varied between 4 and 13 s to investigate if any fast rotation period was obvious and initial measurements indicated a period of ~4 minutes. It was then observed on 2022 July 9.91 UTC for 19 minutes when it had approached to 1.3 LD, had brightened to 15th mag, and was moving at 170 arcsec/min, but at an altitude of 26° or less and in twilight. Exposures were kept to 1 s duration to limit trailing. Over the three nights, 1002 individual images were obtained with exposures ranging from 1 - 13.1 s, but considering the initial determination of the period P at ~4 min and with the optimal exposure Δt for recording a strong signal without excessive smoothing of the resulting lightcurve being $0.185P$ (Pravec et al., 2005), these were then stacked in *Astrometrica* in groups so that the elapsed time from start of the first exposure to end of the last exposure in each stack was 30 s or less, so $\Delta t/P \sim 0.125$. This resulted in 191 stacked measurements being used in the final analysis. The period spectrum shows the best fit solution is indeed close to the initial estimate of P and the resulting asymmetric, bimodal lightcurve indicating P = 0.068406 h = 4.1 min.

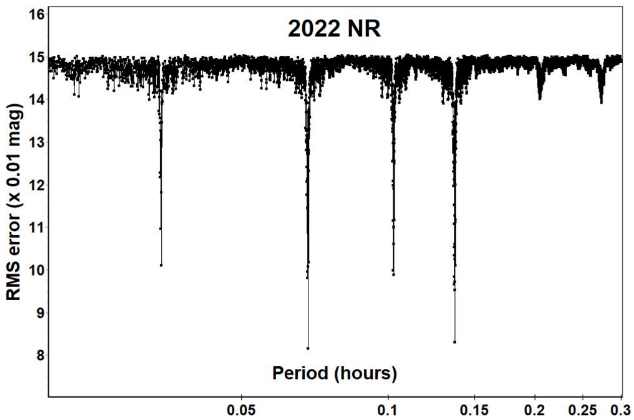

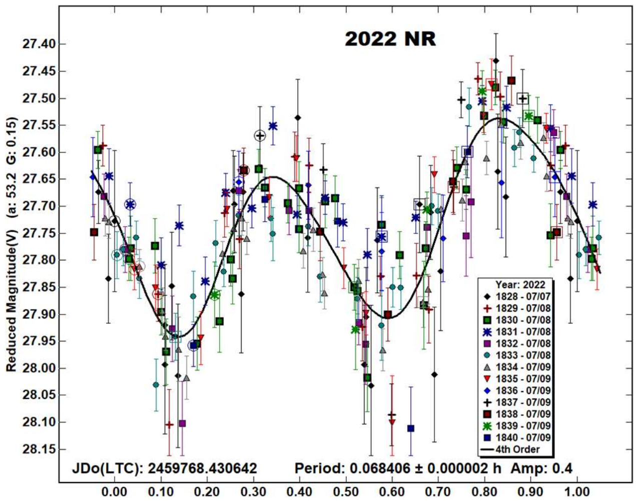

The period indicates that observations on the first night covered 3.7 revolutions, 37 on the second night, and 4.6 on the third night. 2022 NR was also observed by radar from Goldstone and an echo power spectrum is available from observations made on 2022 July 8 (Benner, 2022).

2022 QC. This Apollo was discovered by Pan-STARRS 2 on 2022 Aug 17.49 UTC and subsequently pre-discovery positions were reported by the same team from 11 days earlier (Dupouy et al., 2022). 2022 QC passed Earth at 2.6 LD on 2022 Aug 20.24 UTC and was observed for 7 minutes starting at 2022 Aug 19.92 UTC, then 1.75 h later for a further 25 minutes. A period spectrum shows a strong signal at 0.0337 h and the resulting lightcurve indicates this is a trimodal solution.

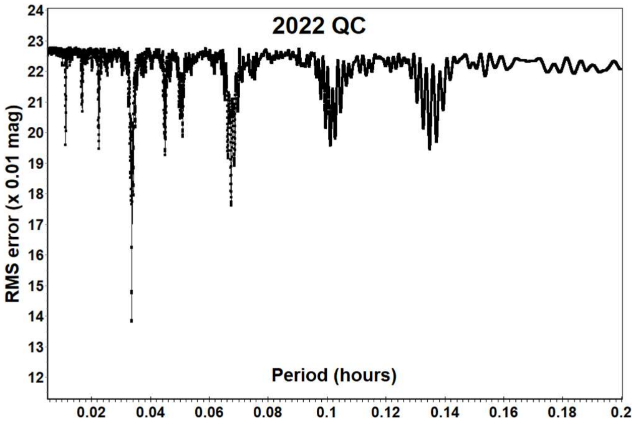

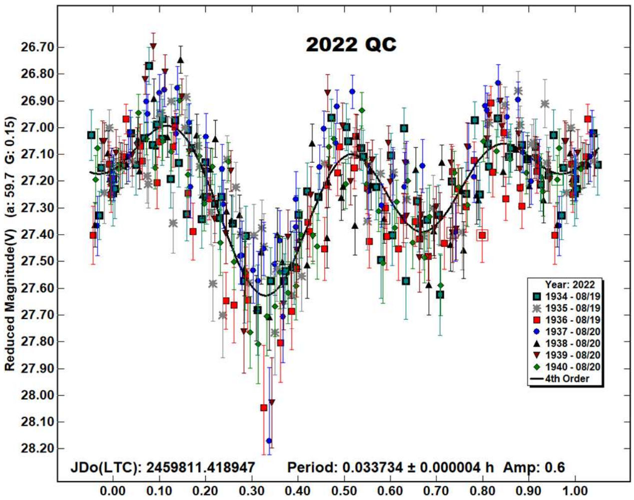

The SBDB listed value of H = 25.29 implies a diameter of approximately 26 m. The rotation period of 121 seconds indicate that 3.6 rotations were observed during the first set of observations and 12 revolutions during the second set.

2022 QV. This was observed for 20 minutes starting on 2022 Aug 21.98 UTC when at a distance of just under 3 LD and moving at 180 arcsec/min. About nine hours later, it passed Earth at 2.2 LD. It had been discovered 2.5 days before by the Pan-STARRS 2 team (Buzzi et al., 2022) and is an Apollo with an approximate diameter of 19 m (H = 26.0). Due to its apparent speed, exposures were limited to 2.8 seconds throughout.

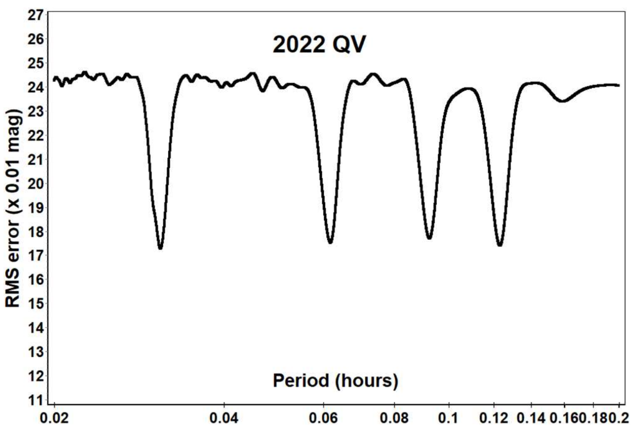

Analysis reveals a bimodal lightcurve with a rotation period of 3.7 minutes, meaning 5.4 revolutions occurred during the observation period.

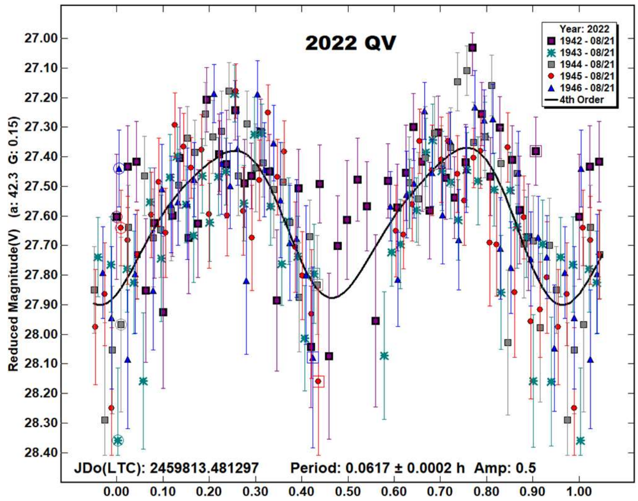

2022 QX4. Discovered by the ATLAS telescope in Chile on 2022 Aug 24 (Melnikov et al., 2022a), this Aten was the subject of some attention in the days after discovery due to an apparent very close approach to Earth in 1977, raising speculation that it might be an artificial object possibly associated with a launch around that time. Pre-discovery images from 2013 Aug were then reported on 2022 Sep 11 (Deen et al., 2022), showing that the effects of solar radiation pressure are negligible and that 2022 QX4 is most likely a natural object. Including the pre-discovery positions, the SBDB now lists 18 approaches to Earth within 10 LD, with an approach on 1977 Sep 5 being the closest, at 0.33 ± 0.01 LD. It was observed for 1.4 h starting 2022 Aug 28.04 UTC at an altitude of only 37° and again for 1.1 h starting 2022 Aug 29.89 UTC at an even lower altitude of 21°. Although the individual sessions were relatively consistent on each night, there was a difference in zero pointing between the two nights of 0.18 magnitudes probably due to the poor observing circumstances and this has been adjusted for in the lightcurve, reducing the overall RMS of the fit from 0.17 to 0.09 mag. A relatively low 0.3 mag amplitude, bimodal lightcurve of period 0.0888 h (5.3 minutes) was determined using *MPO Canopus*. The period spectrum shows the four strongest signals are associated with the 5.3-minute period (monomodal to quadrimodal solutions) but there are several other lesser minima suggesting some tumbling motion may be present, but attempts to resolve a second period using the *MPO Canopus* Dual-Period Search function were unsuccessful.

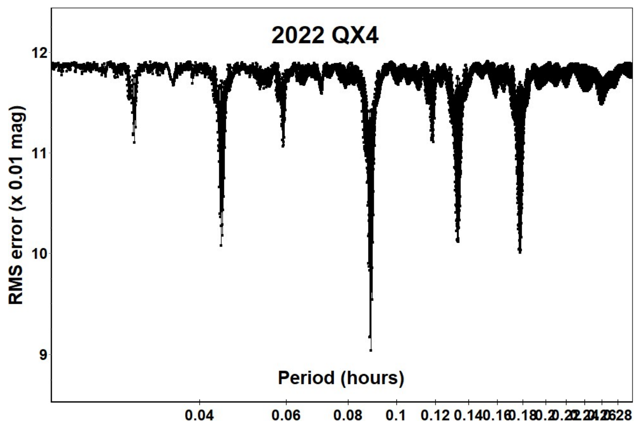

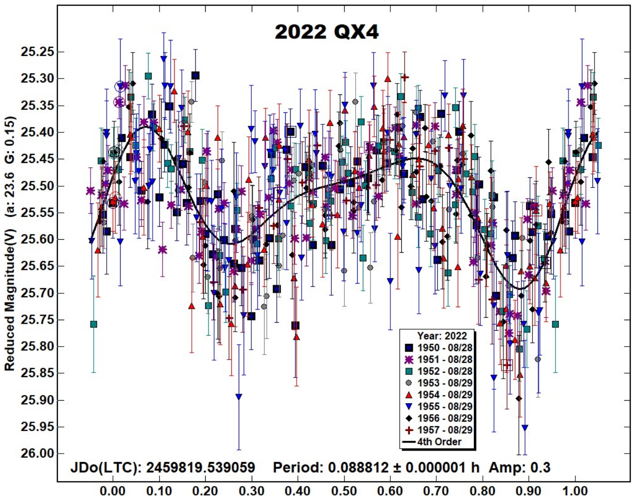

The period indicates that 15 revolutions were observed on the first night of observation and 12 on the second. The low amplitude lightcurve is consistent with 2022 QX4 being a natural object, other distant artificial objects observed from Great Shefford have typically had much larger amplitudes. Assuming it is a natural object, the SBDB value of H = 24.69 suggests a diameter of about 34 m.

2022 QT7. Discovered by Pan-STARRS 2 on 2022 Aug 29.5 UTC, this small Aten (H = 28.6, dia. ~ 6 m) passed Earth at 1.2 LD on 2022 Sep 1.4 UTC (Melnikov et al., 2022b). It was observed for 2.8 h starting on 2022 Aug 31.93 UTC at a distance of 1.5 LD and with its apparent speed increasing to 160 arcsec/minute exposure lengths were kept within the range 3.6 - 5.3 seconds. The average gap between images was 1.5 seconds. Large magnitude variations between consecutive images were evident during capture, with the asteroid sometimes appearing at approximately maximum brightness in one image, then being completely invisible in the next. This can cause problems for lightcurve analysis where a minimum may be poorly recorded, so exceptionally, in an attempt to get at least some definition of deep minima, measurements where the asteroid was visible but with SNr down to 2 were included, allowing 417 data points to be used for the analysis.

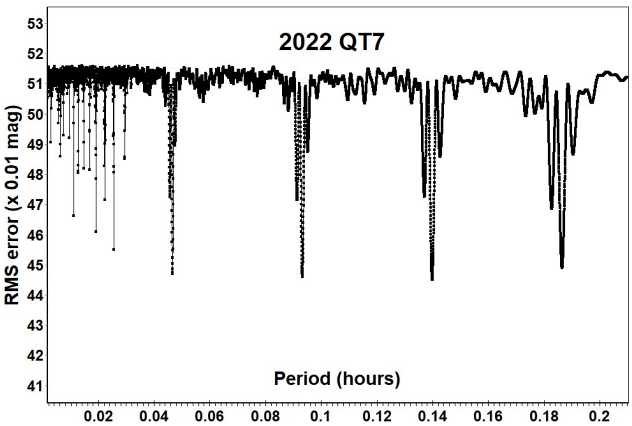

An initial search for rotation periods in the range 0.001 - 0.26 h resulted in the best fit being a bimodal solution with period 0.09327 h, this lightcurve is labelled PAR. Only slightly inferior fits at 0.047, 0.14 and 0.19 h shown on the linearly-scaled period spectrum relate to monomodal, trimodal and quadrimodal versions of the bimodal solution. However, there are obvious problems with the lightcurve, with large scatter even on the measurements with high SNr. It is also apparent that there appear to be a number of RMS minima in the period spectrum below 0.04 h.

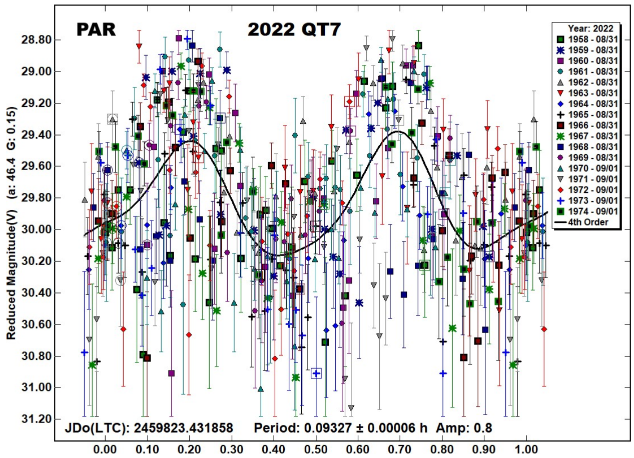

The *MPO Canopus* Dual-Period Search function was then used to search for possible tumbling rotation using 0.09327 h as the initial estimate for the main period. This resulted in improving the fit of the main lightcurve and finding a secondary period of 0.0063789 ± 0.0000003 h (23.0 seconds) and these lightcurves are given, labelled P1 and P2.

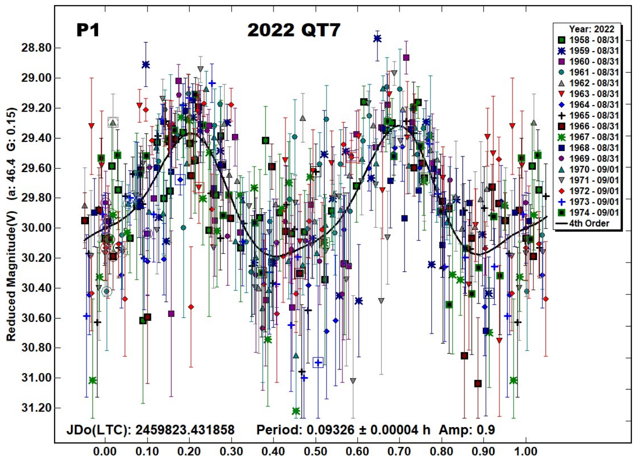

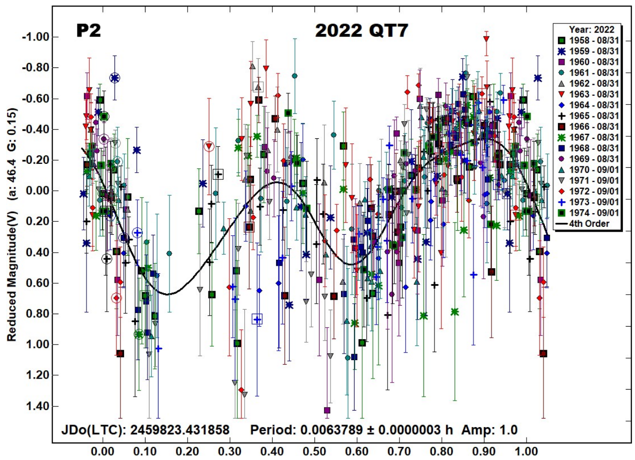

The many RMS minima in the period spectrum below 0.04 h were then examined using the Dual-Period Search to see whether or not the two periods of tumbling motion could be described entirely from those shorter rotation periods. The strongest signal initially located was a close match for the earlier P_2 period and given here labelled as P3. Subtracting the effect of the P_3 lightcurve using the Dual-Period Search produced a period spectrum showing two sets of RMS minima, being multiples of 0.0056096 and 0.0073888 h, (20.2 and 26.6 seconds respectively), with plausible solutions at double these values.

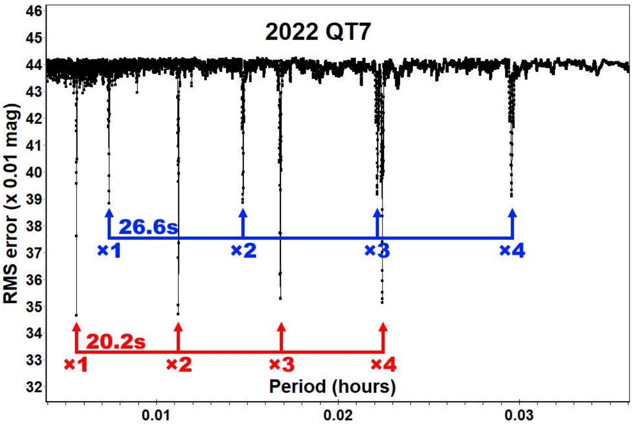

A lightcurve for the best fit solution, at 0.0112204 h is given, labelled P4 and the lesser fit at 0.0147778 h labelled P5.

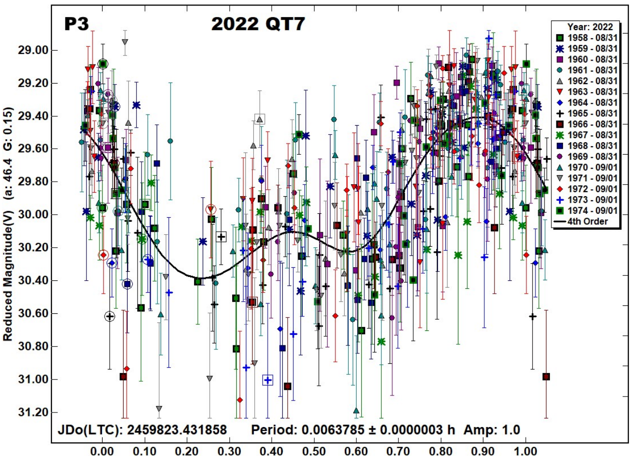

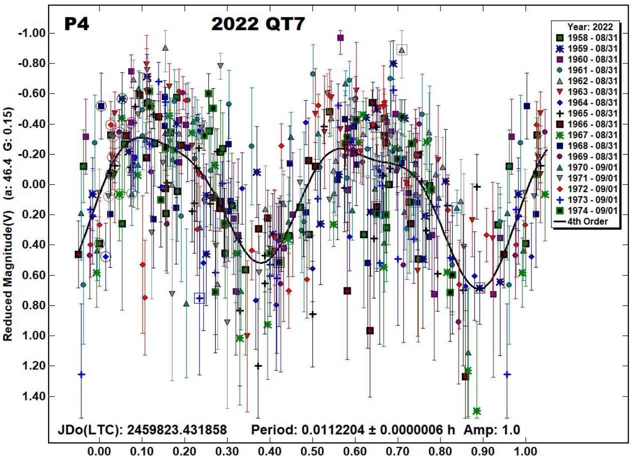

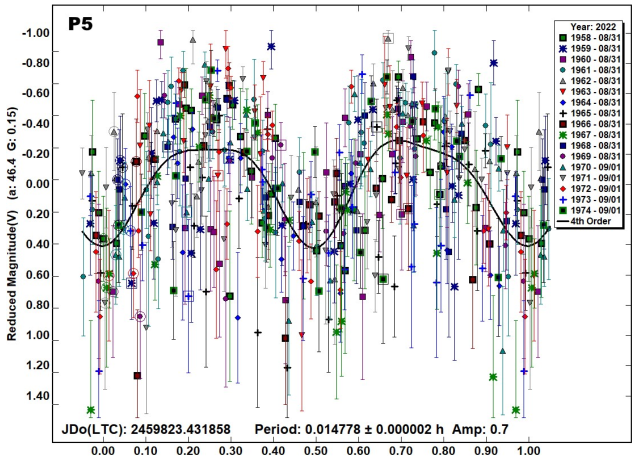

It is noted that the three short periods:

$P_3 = 0.0063785 \pm 0.0000003$ h
$P_4 = 0.0112204 \pm 0.0000006$ h
$P_5 = 0.014778 \quad \pm 0.000002$ h

are related to each other by: $1/P_3 \approx 1/P_4 + 1/P_5$ and that the initially apparent dominant period P_1 of 0.09326 ± 0.00004 h is also related to the shorter periods, e.g.: $2/P_1 \approx 2/P_4 - 1/P_3$.

The P_1 period is expected to be a beat between the two real frequencies of the tumbling motion, the main period is likely to be P_4, but which one of the other periods may be real is not clear. It is expected that the rotation may be rated with a PAR code of -2, tending to -3 on the scale of Pravec et al. (2005) (Petr Pravec, personal communication).

The real amplitude of each of the lightcurves presented is likely to be larger than indicated, due to the asteroid being too faint to record at minimum light. Lightcurve smoothing also needs to be considered for the fastest period P_3 = 22.96 s and longest exposure = 5.3 s. The longest exposure as a fraction of period P_3 is 5.3/22.96 = $0.231P_3$ and this would be expected to cause some appreciable smoothing, with the strength of the second harmonic being reduced to 68% of its true value. However, these exposures only account for 18 of the 417 data points (4.3%), with the remaining exposures being $0.192P$ or less, close to the optimum value of $0.185P$ for a strong detection of the normally dominant second harmonic (Pravec et al., 2000) and so smoothing is not expected to affect the shape of the lightcurves significantly.

2022 SG3. A discovery by Pan-STARRS 2 on 2022 Sep 20.4 UTC, with pre-discovery positions from the day before being reported from the ATLAS Chile site (Bacci et al., 2022a), 2022 SG3 made an approach to 1.7 LD on 2022 Sep 22.3 UTC. It was observed for 2.5 h starting on 2022 Sep 22.02 UTC when it was 16th mag and moving at up to 180 arcsec/minute; exposures were limited to 3.3 seconds or shorter throughout. An initial analysis produced a period spectrum showing a set of solutions in the range of 0.08 - 0.36 h.

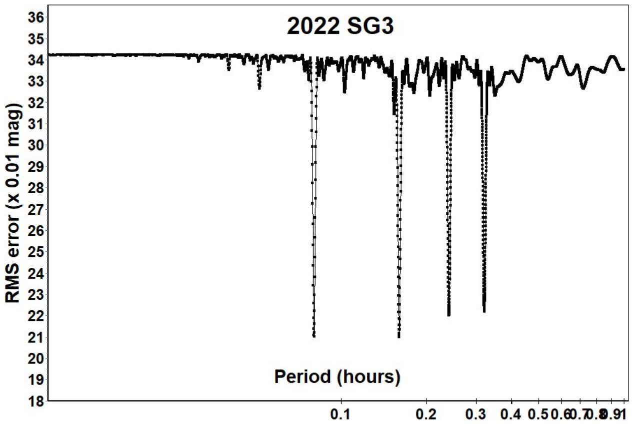

A bimodal lightcurve of period ~0.16 h gave the best fit and is here labelled PAR. The amount of scatter in the brighter parts of the curve was larger than expected and again a dual-period solution was attempted using *MPO Canopus* in case the object is tumbling. When the dominant period of 0.16034 h, amplitude 0.8 was located and subtracted by the Dual-Period Search function it revealed a well-defined secondary period of 0.10306 ± 0.00006 h with amplitude 0.3 mag. These lightcurves are labelled P1 and P2.

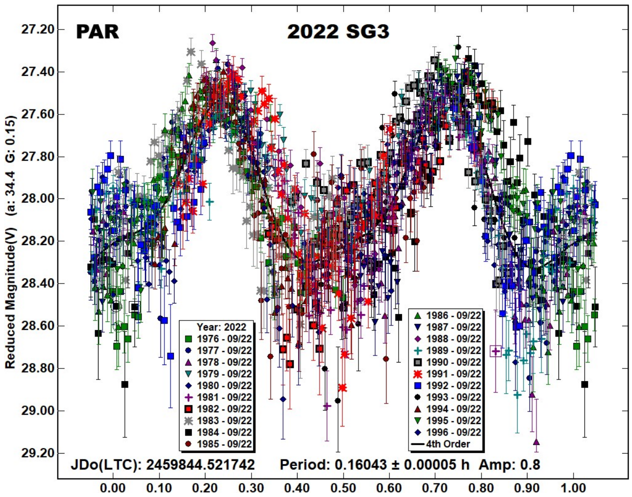

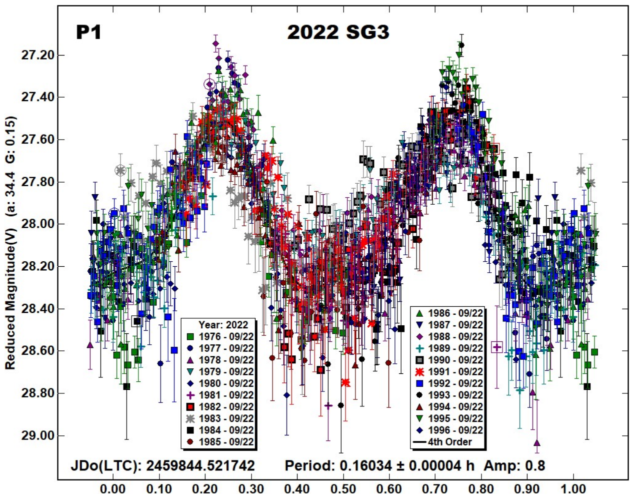

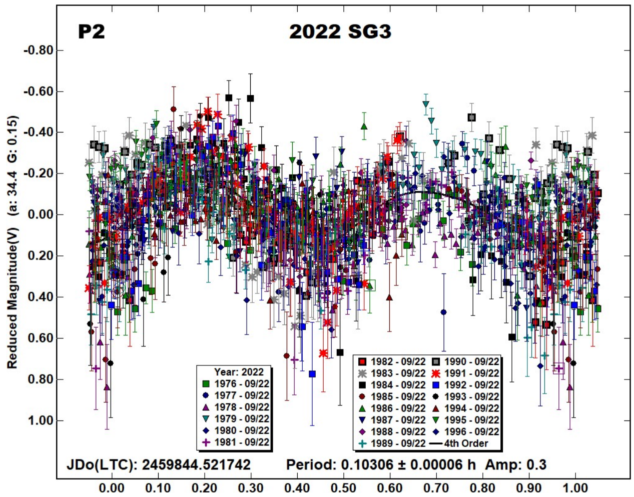

This non-principal axis (NPA) rotation solution is expected to be rated with a PAR code of -3 on the scale of Pravec et al. (2005)., i.e., *NPA rotation reliably detected with the two periods resolved. There may be some ambiguities in one or both periods...*

<u>2022 SW3</u>. This was an amateur discovery from the PASTIS Observatory, Banon, France, on 2022 Sep 20.14 UTC (Bacci et al., 2022b). The SBDB lists this Aten with *H* = 24.84, suggesting an approximate diameter of 32 m. It passed closest to Earth on 2022 Sep 23.2 UTC at 7 LD and was observed over three separate sessions, starting 2022 Sep 23.89, Sep 24.09 and Sep 25.09 UTC for 97, 75 and 102 minutes respectively. Large variations in magnitude were evident over several minutes during each session and an analysis shows a large amplitude bimodal lightcurve. It is noted that with an orbital period of 0.6699 years 2022 SW3 completes almost exactly three revolutions of the Sun every two Earth years and will approach to a similar distance of 7 LD from Earth on 2024 Sep 19, though not as well placed as in 2022, but then will not approach any closer until 2077.

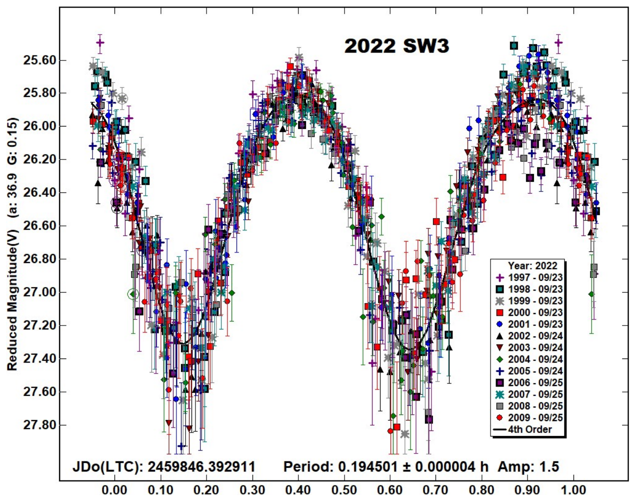

Name	2022 mm/ dd	Phase	L_{PAB}	B_{PAB}	Period(h)	P.E.	Amp	A.E	PAR	H
2022 NE	07/05-07/06	31.8-31.7	269	6	0.015488	0.000004	1.0	0.3	-3	28.65
					0.02005	0.00001	0.6	0.3		
					0.01217	0.00001	0.4	0.4		
2022 NR	07/07-07/09	53.1-65.3	262	14	0.068406	0.000002	0.4	0.1		25.87
2022 QC	08/19-08/20	59.6-66.6	351	22	0.033734	0.000004	0.6	0.2		25.30
2022 QV	08/21-08/21	42.3-42.9	350	2	0.0617	0.0002	0.5	0.2		25.95
2022 QX4	08/28-08/29	23.6-19.5	336	0	0.088812	0.000001	0.3	0.1		24.69
2022 QT7	08/31-09/01	46.4-51.1	358	15	0.0112204	0.0000006	1.0	0.5	-2/-3	28.59
					0.0063785	0.0000003	1.0	0.5		
					0.0147778	0.0000015	0.7	0.5		
2022 SG3	09/22-09/22	34.2-41.4	16	8	0.16034	0.00004	0.8	0.3	-3	27.05
					0.10306	0.00006	0.3	0.3		
2022 SW3	09/23-09/25	36.9-34.8	11	15	0.194501	0.000004	1.5	0.3		24.84

Table I. Observing circumstances and results. The phase angle is given for the first and last date. If preceded by an asterisk, the phase angle reached an extrema during the period. LPAB and BPAB are the approximate phase angle bisector longitude/latitude at mid-date range (see Harris et al., 1984). Amplitude error (A.E.) is calculated as √2 * (lightcurve RMS residual). PAR is the expected Principal Axis Rotation quality detection code (Pravec et al., 2005) and H is the absolute magnitude at 1 au from Sun and Earth taken from the Small-Body Database Lookup (JPL, 2022).

Acknowledgements

The author is indebted to Petr Pravec for help and encouragement in the analysis of the tumblers 2022 NE, 2022 QT7 and 2022 SG3. Also gratefully acknowledged is a Gene Shoemaker NEO Grant from the Planetary Society (2005) and a Ridley Grant from the British Astronomical Association (2005), both of which facilitated upgrades to observatory equipment used in this study.

References

ADS (2022). Astrophysics Data System. *https://ui.adsabs.harvard.edu/*

Bacci, P.; Maestripieri, M.; Tesi, L.; Fagioli, G.; Foglia, S.; Galli, G.; Buzzi, L.; Pettarin, E.; Dupouy, P.; de Vanssay, J.B.; Camarasa, J.; Duszanowicz, G.; Bulger, J.; Lowe, T.; Schultz, A. and 38 colleagues (2022a). "2022 SG3." *MPEC 2022-S101. https://minorplanetcenter.net/mpec/K22/K22SA1.html*

Bacci, P.; Maestripieri, M.; Tesi, L.; Fagioli, G.; Dupouy, P.; de Vanssay, J.B.; Camarasa, J.; Duszanowicz, G.; Holmes, R.; Linder, T.; Horn, L.; Losse, F.; Demeautis, C.; Attard, G.; Maury, A. and 2 colleagues (2022b). "2022 SW3." *MPEC 2022-S116. https://minorplanetcenter.net/mpec/K22/K22SB6.html*

Name	Integration times	intg/Pd	Max Min a/b	Pts	Flds
2022 NE	5	0.114	2.1	310	4
2022 NR	30Σ	0.122	1.1*	191	13
2022 QC	2.7	0.022	1.2*	375	7
2022 QV	2.8	0.013	1.2*	228	5
2022 QX4	11.1	0.035	1.2	450	8
2022 QT7	5.3	0.231	1.9*	417	17
2022 SG3	3.3	0.009	1.6*	1266	21
2022 SW3	16.4	0.023	2.0	775	13

Table II. Ancillary information, listing the integration times used (seconds), the fraction of the period represented by the longest integration time (Pravec et al., 2000), the calculated minimum elongation of the asteroid (Zappala et al., 1990), the number of data points used in the analysis and the number of times the telescope was repositioned to different fields. Note: Σ = Longest elapsed integration time for stacked images (start of first to end of last exposure used), * = Value uncertain, based on phase angles > 40°.

Benner, L.A.M. (2022). "Goldstone Radar Observations Planning: 1994 AW1, 2022 NR, Tukmit, and 2006 YT13." *https://echo.jpl.nasa.gov/asteroids/1994AW1/1994AW1.2022.goldstone.planning.html*

Buzzi, L.; Linder, T.; Holmes, R.; Horn, L.; Bulger, J.; Chambers, K.; Lowe, T.; Schultz, A.; Smith, I.; Chastel, S.; Fairlamb, J.; Huber, M.; Ramanjooloo, Y.; Wainscoat, R.; Weryk, R. and 14 colleagues (2022). "2022 QV." *MPEC 2022-Q42. https://minorplanetcenter.net/mpec/K22/K22Q42.html*

Deen, S.; Sanchez, S.; Nomen, J.; Hurtado, M.; Jaume, J.A.; Yeung, W.K.Y.; Serra, F.; Valls, T.; Hurtado, J.; Micheli, M. (2022). "2022 QX4." *MPEC 2022-R148. https://minorplanetcenter.net/mpec/K22/K22RE8.html*

Dupouy, P.; Bulger, J.; Chambers, K.; Dukes, T.; Lowe, T.; Schultz, A.; Smith, I.; Chastel, S.; Fairlamb, J.; Huber, M.; Ramanjooloo, Y.; Wainscoat, R.; Weryk, R.; de Boer, T.; Gao, H. and 4 colleagues (2022). "2022 QC." *MPEC 2022-Q16. https://minorplanetcenter.net/mpec/K22/K22Q16.html*

Evans, N.; Choi, P.; Saini, N.; Zhai, C.; Trahan, R.; Shao, M.; Linder, T.; Holmes, R.; Horn, L.; Bulger, J.; Lowe, T.; Schultz, A.; Smith, I.; Chambers, K.; Dukes, T. and 11 colleagues (2022). "2022 NE." *MPEC 2022-N29. https://minorplanetcenter.net/mpec/K22/K22N29.html*

Fazekas, J.B.; Christensen, E.J.; Fay, D.; Fuls, D.C.; Gibbs, A.R.; Grauer, A.D.; Groeller, H.; Hogan, J.K.; Kowalski, R.A.; Larson, S.M.; Leonard, G.J.; Rankin, D.; Seaman, R.L.; Serrano, A.; Shelly, F.C. and 27 colleagues (2022). "2022 NR." *MPEC 2022-N43. https://minorplanetcenter.net/mpec/K22/K22N43.html*

Harris, A.W.; Young, J.W.; Scaltriti, F.; Zappala, V. (1984). "Lightcurves and phase relations of the asteroids 82 Alkmene and 444 Gyptis." *Icarus* **57**, 251-258.

Harris, A.W.; Young, J.W.; Bowell, E.; Martin, L.J.; Millis, R.L.; Poutanen, M.; Scaltriti, F.; Zappala, V.; Schober, H.J.; Debehogne, H.; Zeigler, K. (1989). "Photoelectric Observations of Asteroids 3, 24, 60, 261, and 863." *Icarus* **77**, 171-186.

JPL (2022). Small-Body Database Lookup. *https://ssd.jpl.nasa.gov/tools/sbdb_lookup.html*

Melnikov, S.; Hoegner, C.; Laux, U.; Ludwig, F.; Stecklum, B.; Holmes, R.; Linder, T.; Horn, L.; Hug, G.; Korlevic, K.; Dusevic, P.; Markovic, M.; Paleka, I.; Perovic, I.; Pettarin, E. and 14 colleagues (2022a). "2022 QX4." *MPEC 2022-Q123*. *https://minorplanetcenter.net/mpec/K22/K22QC3.html*

Melnikov, S.; Hoegner, C.; Laux, U.; Ludwig, F.; Stecklum, B.; Bulger, J.; Lowe, T.; Schultz, A.; Smith, I.; Chambers, K.; Dukes, T.; Chastel, S.; de Boer, T.; Fairlamb, J.; Gao, H., and 22 colleagues (2022b). "2022 QT7." *MPEC 2022-Q189*. *https://minorplanetcenter.net/mpec/K22/K22QI9.html*

Pravec, P.; Hergenrother, C.; Whiteley, R.; Sarounova, L.; Kusnirak, P.; Wolf, M. (2000). "Fast Rotating Asteroids 1999 TY2, 1999 SF10, and 1998 WB2." *Icarus* **147**, 477-486.

Pravec, P.; Harris, A.W.; Scheirich, P.; Kušnirák, P.; Šarounová, L.; Hergenrother, C.W.; Mottola, S.; Hicks, M.D.; Masi, G.; Krugly, Yu.N.; Shevchenko, V.G.; Nolan, M C.; Howell, E.S.; Kaasalainen, M.; Galád, A., and 5 colleagues. (2005). "Tumbling Asteroids." *Icarus* **173**, 108-131.

Raab, H. (2018). Astrometrica software, version 4.12.0.448. *http://www.astrometrica.at/*

Warner, B.D.; Harris, A.W.; Pravec, P. (2009). "The Asteroid Lightcurve Database." *Icarus* **202**, 134-146. Updated 2021 Dec. *https://minplanobs.org/mpinfo/php/lcdb.php*

Warner, B.D. (2022). MPO Software, Canopus version 10.8.6.9. Bdw Publishing, Eaton, CO. *http://minorplanetobserver.com*

Zacharias, N.; Finch, C.T.; Girard, T.M.; Henden, A.; Bartlett, J.L.; Monet, D.G.; Zacharias, M.I. (2013). "The Fourth US Naval Observatory CCD Astrograph Catalog (UCAC4)." *Astronomical Journal* **145**, 44-57.

Zappala, V.; Cellini, A.; Barucci, A.M.; Fulchignoni, M.; Lupishko, D.E. (1990). "An analysis of the amplitude-phase relationship among asteroids." *Astron. Astrophys.* **231**, 548-560.

LIGHTCURVE ANALYSIS OF HILDA ASTEROIDS AT THE CENTER FOR SOLAR SYSTEM STUDIES: 2022 JULY-OCTOBER

Brian D. Warner
Center for Solar System Studies (CS3)
446 Sycamore Ave.
Eaton, CO 80615 USA
brian@MinorPlanetObserver.com

Robert D. Stephens
Center for Solar System Studies (CS3)
Rancho Cucamonga, CA

(Received: 2022 October 7)

CCD photometric observations of eight Hilda asteroids were made at the Center for Solar System Studies between 2022 July and October.

CCD photometric observations of eight Hilda asteroids were carried out at the Center for Solar System Studies (CS3) from 2022 July-October as part of an ongoing study of the family/group that is located between the outer main-belt and Jupiter Trojans in a 3:2 orbital resonance with Jupiter. The goal is to determine the spin rate statistics of the Hildas and to find pole and shape models when possible. We also look to examine the degree of influence that the YORP (Yarkovsky-O'Keefe-Radzievskii-Paddack) effect (Rubincam, 2000) has on distant objects and to compare the spin rate distribution against the Jupiter Trojans, which can provide evidence that the Hildas are more "comet-like" than main-belt asteroids.

Telescopes	Cameras
0.30-m *f*/6.3 Schmidt-Cass	FLI Microline 1001E
0.35-m *f*/9.1 Schmidt-Cass	FLI Proline 1001E
0.35-m *f*/11 Schmidt-Cass	SBIG STL-1001E
0.40-m *f*/10 Schmidt-Cass	
0.50-m *f*/8.1 Ritchey-Chrétien	

Table I. List of available telescopes and CCD cameras at CS3. The exact combination for each telescope/camera pair can vary due to maintenance or specific needs.

Table I lists the telescopes and CCD cameras that are available to make observations. All the cameras use CCD chips from the KAF 1001 blue-enhanced family and so have essentially the same response. The pixel scales ranged from 1.24-1.60 arcsec/pixel. All lightcurve observations were unfiltered or with a clear filter, even though the latter can result in a 0.1-0.3 magnitude loss. The exposures varied depending on the asteroid's brightness.

To reduce the number of times and amounts of adjusting nightly zero-points, the ATLAS catalog r´ (SR) magnitudes (Tonry et al., 2018) are used. Those adjustments are usually ≤ ±0.03 mag. The rare greater corrections may have been related in part to using unfiltered observations, poor centroiding of the reference stars, and not correcting for second-order extinction. Another cause may be selecting what appears to be a single star but is actually an unresolved pair.

The Y-axis values are ATLAS SR "sky" (catalog) magnitudes. The values in the parentheses give the phase angle(s), *a*, and the value of *G* used to normalize the data to the comparison stars used in the earliest session. This, in effect, corrects all the observations so that seem to have been made at a single fixed date/time and phase angle,